Polymer 99 (2016) 222–230

Contents lists available at ScienceDirect

Polymer

journal homepage: www.elsevier.com/locate/polymer

Deformation mechanisms in ionic liquid spun cellulose fibers

Nandula D. Wanasekara [a], Anne Michud [b], Chenchen Zhu [c], Sameer Rahatekar [c], Herbert Sixta [b], Stephen J. Eichhorn [a, *]

[a] College of Engineering, Maths and Physical Sciences, Harrison Building, North Park Road, University of Exeter, UK
[b] Department of Forest Products Technology, Aalto University, P.O. Box 16300, Vuorimiehentie 1, Espoo, FI-00076, Finland
[c] Advanced Composites Centre for Innovation and Science (ACCIS), Aerospace Engineering, University of Bristol, Bristol, UK

ARTICLE INFO

Article history:
Received 4 May 2016
Received in revised form
21 June 2016
Accepted 1 July 2016
Available online 5 July 2016

Keywords:
Cellulose
Fibers
Molecular deformation

ABSTRACT

The molecular deformation and crystal orientation of a range of next generation regenerated cellulose fibers, produced from an ionic liquid solvent spinning system, are correlated with macroscopic fiber properties. Fibers are drawn at the spinning stage to increase both molecular and crystal orientation in order to achieve a high tensile strength and Young's modulus for potential use in engineering applications. Raman spectroscopy was utilized to quantify both molecular strain and orientation of fibers deformed in tension. X-ray diffraction was used to characterize crystal orientation of single fibers. These techniques are shown to provide complimentary information on the microstructure of the fibers. A shift in the position of a characteristic Raman band, initially located at ~1095 cm^{-1}, emanating from the backbone structure of the cellulose polymer chains was followed under tensile deformation. It is shown that the shift rate of this band with respect to strain increases with the draw ratio of the fibers, indicative of an increase in the axial molecular alignment and subsequent deformation of the cellulose chains. A linear relationship between the Raman band shift rate and the modulus was established, indicating that the fibers possess a series aggregate structure of aligned crystalline and amorphous domains. Wide-angle X-ray diffraction data show that crystal orientation increases with an increase in the draw ratio, and a crystalline chain slip model was used to fit the change in orientation with fiber draw ratio. In addition to this a new model is proposed for a series aggregate structure that takes into better account the molecular deformation of the fibers. Using this model a prediction for the crystal modulus of a cellulose-II structure is made (83 GPa) which is shown to be in good agreement with other experimental approaches for its determination.

1. Introduction

The history of commercial regenerated cellulose fiber technology goes back to 1892 when the first patent was granted for a method for the improvement in dissolving cellulose [1].Later on, this method of cellulose dissolution became widely known as the 'viscose process'. With the establishment of the first commercial viscose plant in 1905, the technology achieved greater success in producing cotton-like fibers. However, the use of aggressive solvents like carbon disulfide presented significant health and safety risks. These problems continued to exist when the viscose process produced high stiffness fibers (called Cordenka™) by the addition of formaldehyde to the spinning dope. These fibers however further suffered from problems related to poor spin-bath recovery. Research efforts to find green solvents for cellulose dissolution resulted in the rediscovery of ionic liquids (ILs) as good solvents for cellulose by Rogers et al. [2] in 2002. The initial development of ionic liquids for cellulose dissolution was targeted to reduce or eliminate undesirable solvents while allowing for flexibility and increased solution efficiency. A new class of next-generation regenerated cellulose fibers named Ioncell have recently been developed by Sixta et al. [3] utilizing a novel ionic liquid solvent 1,5-diazabicyclo [4.3.0]non-5-enium acetate ([DBNH] [OAc]). Ioncell fibers have been shown to exhibit higher tenacity than commercial viscose and lyocell fibers [4] owing to the milder process conditions and high degree of chain alignment along the fiber axis [5].

There have been extensive studies on molecular and crystal deformation of other, more conventional regenerated cellulose

* Corresponding author. College of Engineering, Maths & Physical Sciences, North Park Road, University of Exeter, Exeter, Devon, EX4 4QF, UK.
E-mail address: s.j.eichhorn@exeter.ac.uk (S.J. Eichhorn).

http://dx.doi.org/10.1016/j.polymer.2016.07.007

fibers. Investigations on NMMO (N-methylmorpholine N-oxide)-based regenerated cellulose fibers have shown that skin-core differences exist in the degree of preferred orientation of crystals [6] and that they possess a radial texture [7]. Another study [8] on lyocell fibers produced using different drawing conditions has shown that both molecular and crystal orientation increase with draw ratio. Further, it was reported that the crystal modulus appears to change with increasing draw ratio [8]. Kong and Eichhorn [9] have investigated the intermolecular hydrogen bonding in regenerated cellulose fibers showing that their breakdown during deformation could be the potential cause of the yield point in the mechanics of the fibers.

Ionic liquid dissolved cellulose offers a potentially more environmentally friendly alternative to traditional processing routes for fibers such as the viscose process. The potential to use this route for the production of high performance cellulose fibers has not been fully explored. A number of studies have however been devoted to understanding the molecular and crystal orientation and deformation of traditional high performance regenerated cellulose fibers [6,10–13]. There is a need to also understand the micromechanics of this new range of ionic liquid spun fibers. Better understanding of molecular deformation and its relationship to the structure of the fibers will ultimately lead to enhanced properties. Here, we have followed the deformation micromechanics and both molecular and crystal orientation to gain insight into the microstructural evolution of Ioncell fibers – a new class of regenerated cellulose fibers.

Raman spectroscopy has been used as an effective tool to understand the molecular deformation of cellulose fibers [10,11,13]. The principle of the technique is based on following a shift in the position of a band that is characteristic of the molecular signature of the polymer backbone, towards a lower wavenumber, upon uniaxial tensile deformation. The discovery of this effect was made by Mitra et al. [14] in 1977 when they followed a shift in the position of a Raman band located at ~1498 cm^{-1} (corresponding to the −C═C− moiety) of conjugated polydiacetylene single crystal fibers under stress. Similar Raman band shifts can be used to understand the mechanics of cellulose fibers and give insights into their molecular deformation mechanisms. Many man-made polymeric fibers [15] and an array of regenerated cellulose fibers [10,16] have been investigated using this technique; in cellulose fibers by following the a characteristic Raman band located at ~1095 cm^{-1} which corresponds to heavy atom modes (−C−C−, −C−O−) [17,18]. This band has also been assigned to the β-1,4-glycosidic linkage (−C-O−C-) between the glucose rings of the cellulose molecules [19].

Complementary use of X-ray diffraction enables the development of a complete picture of the crystallite orientation and deformation of cellulose fibers. Small angle X-ray scattering (SAXS) has been used to obtain skin-core characteristics of pore geometries and crystal orientation in lyocell fibers [20], in addition to the use of Raman spectroscopy to follow molecular deformation [9,13]. Gindl et al. [6] used X-ray diffraction to analyze the orientation of bent lyocell fibers, showing that in a loop test the upper-side of the fibers, which was in tension, exhibited an increase in orientation compared to the under-side, which was in compression. Further, it has been shown that highly drawn regenerated cellulose fibers exhibit a greater degree of crystal orientation than fibers produced with relatively less tension [6].

Although there have been a few studies [21,22] on ionic liquid spun fibers, the structure-property relationships and deformation mechanics at the molecular level are not well understood. The novelty of this work stems from the need to better understand the molecular deformation and orientation of ionic liquid spun cellulose fibers and more importantly, critically assess the ways to improve the modulus of the fibers further. In order to increase the elastic modulus and tensile strength of fibers, a reduction of chemical (non-cellulosic compounds) and physical (structural defects) impurities in the fibers and an increase in the total molecular and crystal orientation may be required. Critical to the enhancement of modulus is to minimize the skin-core differences that exist in the degree of preferred orientation of crystals [6,23]. A more uniform orientation of molecules and crystals in both skin and core is likely to result in enhanced elastic modulus.

In this study, we report on the molecular deformation and crystal orientation of Ioncell cellulose fibers. These fibers differ from conventionally spun regenerated cellulose filaments in that they use a “green” IL solvent, and therefore could be a credible and sustainable alternative. We show that orientation of the molecular chains and crystalline structure of the cellulose plays a role in dictating their high mechanical properties. Although our results concur with previously published work [13] we use a new model to describe the molecular deformation of the fibers. This model is combined with conventional theories of uniform stress microstructures, but critically deviates significantly from previous series aggregate approaches to the deformation of polymer fibers. Using this new approach we are able to predict the crystal modulus of the fibers, showing that there is good agreement with other experimental results, and setting a benchmark for achieving yet higher mechanical properties for our fibers.

2. Experimental methods

2.1. Materials

Birch pre-hydrolysis Kraft pulp from Stora Enso Enocell pulp mill in Finland was used as the cellulosic solute as previously described [4]. This cellulose pulp was received in sheet form and was grounded to a powder form using a Wiley mill prior to dissolution. The intrinsic viscosity was 476 ml g^{-1} and number average molecular weight (Mn) of Enocell cellulose was determined to be 65.9 kg mol^{-1}. The production process for this fiber has been described in detail elsewhere [4]. In brief, cellulose was dissolved in [DBNH][OAc] using several steps; firstly [DBNH][OAc] was liquefied at 70 °C in a water bath and subsequently liquefied [DBNH][OAc] and cellulose (13 wt%) were mixed to obtain a homogenous slurry. This slurry was then transferred to a vertical kneader (80 °C, 10 rpm, 100 mbar for 75 min) where the dissolution takes place. The resulting dope was filtrated using a hydraulic pressure filtration unit at 80 °C to remove any undissolved impurities. The resulting dope was highly viscous and was shaped into a cylinder and stored under refrigeration for a few days for solidification.

2.2. Fiber production

A customized laboratory piston-spinning unit (Fourné Polymertechnik, Germany) was used to spin multi-filaments. The cylinder shaped cellulose was heated back to 80 °C in order to obtain a homogeneous spinning solution. The fiber extrusion was conducted through a multi-hole spinneret at moderate temperature (80 °C) into a water coagulation bath via an air gap. The extrusion velocity (5.7 m min^{-1}) was kept constant and the take-up velocity was increased to obtain fibers with a range of draw ratios. Finally, the fibers were washed offline using hot water for 1 h at 70 °C and air-dried without tension.

2.3. Raman spectroscopy

A Renishaw 1000 Raman spectrometer with an imaging

microscope equipped with a thermoelectrically cooled CCD detector was utilized to record spectra. A near-IR laser with a wavelength of 785 nm was used to record spectra from single Ioncell fibers using an exposure time of 30 s and two accumulations. The laser beam was focused using a 50 × objective lens to a spot size of ~1–2 μm. To obtain molecular orientation profiles a single fiber was placed with its major axis parallel to the polarization direction of the laser, under the microscope of the Raman spectrometer. Both incident and scattered light radiation was polarized parallel to the principle axis of the Raman spectrometer and the major axis of the fiber. The polarization direction of the incident light was changed incrementally using a half-wave plate, and a fixed polarizer was used to maintain the polarization direction of scattered light parallel to the fiber axis. The intensity of a characteristic Raman band located at ~1095 cm^{-1} was recorded as a function of the rotation angle of the incoming polarizer with respect to the axis of the fibers. As before, a Lorentzian function was utilized to fit Raman peaks in order to find their intensities. The maximum intensity was determined from the most intense peak from which a normalization of other intensities was performed.

2.4. X-ray diffraction

Wide Angle X-ray Diffraction (WAXD) patterns of Ioncell fibers were obtained with an exposure time of 5 h, using a SAXSLAB GANESHA 300 XL SAXS system in the School of Physics at the University of Bristol. Cu Kα radiation with a wavelength of 0.154 nm was used. In order to process the data, reduction and analysis software (SAXSGUI) was used. A single fiber sample was mounted straight and tight on a sample holder, which was located on the sample stage between the X-ray generator and the detector. Experiments were repeated with a bundle of fibers to obtain more signal from the diffracted beam.

2.5. Mechanical properties

Fiber linear density measurement (dtex) and tensile testing of single fibers was carried out using a Vibroskop-Vibrodyn system (Lenzing Instruments GmbH & Co KG, Austria) to determine the Young's modulus, tensile strength (obtained from tenacity cN tex^{-1}) and elongation at break (%). Ten fiber samples for each draw ratio were tested in a conditioned state at 23°C and 50% humidity. A gauge length of 20 mm and a speed of 20 mm min^{-1} were used for tensile testing as per the guidelines in DIN 53816. Young's modulus of Ioncell fibers was calculated using a MATLAB script written according to ASTM standard D2256/D2256 M.

For molecular deformation studies on single fibers the same Raman spectrometer described previously was used. Samples were secured to fiber testing cards as previously described [17] and were deformed in tension using a Deben deformation rig equipped with a 20 N load cell. This deformation rig was carefully placed onto the stage of a Leica microscope, which is attached to the Raman spectrometer. The incident and scattered radiation was polarized parallel to the principle axis of the fibers. The polarization direction of the incident light was rotated using a half-wave plate, and a polarizer was used to maintain the polarization direction of scattered light parallel to the axis of the cellulose fibers. The precise positions of the Raman band initially located at ~1095 cm^{-1} were recorded as a function of the tensile deformation of the fibers. A Lorentzian function was used to fit the Raman peaks in order to locate their positions, and intensities.

3. Results and discussion

3.1. Molecular and crystal structure of fibers

Raman spectroscopy and X-ray diffraction were used to follow molecular and crystal orientation, respectively. A typical Raman spectrum obtained from a single Ioncell fiber is shown in Fig. 1; data are plotted in the region between 800 and 1600 cm^{-1} highlighting the position of a very intense band located at ~1095 cm^{-1}.

Wiley and Atalla [18] have made approximate Raman band assignments for a cellulose-II structure, assigning the intense band located at ~1095 cm^{-1} to the C–O ring stretch modes; others [13] have assigned this band to the glycosidic ring stretch (C–O–C). The change in the intensity of the Raman band located at ~1095 cm^{-1} can be used to map the orientation of molecules relative to the long axis of the fiber, provided the laser radiation exciting the vibration is polarized parallel to this axis. Polar plots of the intensity of this band as a function of the rotational angle of the polarizer are presented to determine the orientation of cellulose chains along the fibers' axes (Fig. 3). The ratio of the intensity of the band located at ~1095 cm^{-1} recorded at 0°, to the intensity of the same band at 90° ($I_{0°}/I_{90°}$) can be used to characterize this degree of molecular alignment. The values of $I_{0°}/I_{90°}$ are 3, 2, 2.5 and 2 for draw ratios 1, 1.5, 3 and 6 respectively, and $I_{0°}/I_{90°}$ are 1.6 for draw ratios 9, 12 and 15. Unexpectedly, the values of $I_{0°}/I_{90°}$ are higher for fibers produced using a low draw ratio than for those produced using higher draw ratios. This result may be interpreted in terms of a skin-core structure to the cellulose fibers, a property of regenerated cellulose fibers that has been reported previously [20]. For instance, the fiber produced using a draw ratio of 1 results in a filament diameter of ~39 μm. Given that the laser spot is ~1–2 μm, with a penetration depth of similar magnitude, means that only the outer skin of these fibers contributes to the Raman signal and thus shows a high molecular orientation ($I_{0°}/I_{90°} = 3$, Fig. 2a). For fibers produced using a higher draw ratio their diameter is smaller e.g. ~11 μm for a draw ratio of 15. As illustrated in Fig. 2, this means that for a given skin-core orientation distribution in the fibers, an average signal from a smaller diameter will result in a lower value of $I_{0°}/I_{90°}$. In addition to this the fibres themselves are virtually transparent to the laser, and so for a given penetration depth one might expect the laser to be sampling a different proportion of the

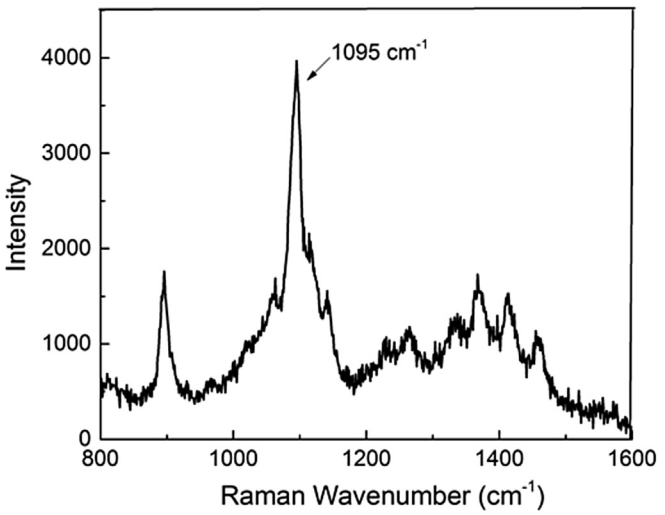

Fig. 1. Typical Raman spectrum for Ioncell cellulose fibers. A characteristic Raman peak for cellulose located at ~1095 cm^{-1} is highlighted.

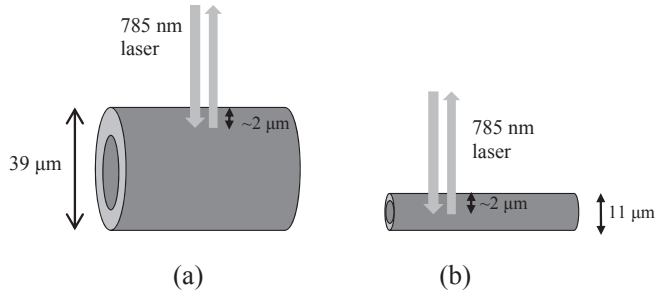

Fig. 2. Schematic that illustrates the effect of a skin-core structure on the Raman signal for a fiber with draw ratios (a) 1 and (b) 15.

orientation distribution. For a larger fibre size there is more attenuation of the laser, and so we believe that data are only being obtained from the outer layer of the fibres, where the polymer chains are more oriented. For a smaller fibre, more of an averaging of the orientation from both the skin and the core is possibly observed.

The orientation polar plots were fitted with the equation

$$I = r + t\cos^4\theta \tag{1}$$

where r and t are fitting parameters, θ is the rotation angle and I is the intensity. It has been reported [24] that Equation (1) can be used to fit orientation data for graphene oxide nanocomposites.

The orientation parameter $\langle\sin^2\theta\rangle$ was calculated from wide angle X-ray scattering data. Typical X-ray diffraction patterns of Ioncell single fibers are shown in Fig. 4. The X-ray beam spot size is 0.8 mm which is much larger than the diameter of a single fiber, therefore the X-ray diffraction patterns from fibers produced with all draw ratios are also taken from bundles of fibers to enhance the intensity of the diffraction signal (see Supplementary Information). The diffraction signal from single fibers are considered for the calculation of $\langle\sin^2\theta\rangle$ to avoid errors of averaging the signal over a wider distribution of crystal orientations and the effects from fibers that may not be straight within the bundles. The arced equatorial reflections that are visible in fibers produced using a low draw ratio (DR = 1.5; Fig. 4a) sharpen for fibers produced using a higher draw ratio 15 (Fig. 4b). These images provide qualitative evidence of higher alignment of crystalline cellulose domains in fibers produced using higher draw ratios. This provides additional evidence that the orientation of the fibers does indeed increase with draw ratio, and should be used in comparison with the data obtained by Raman spectroscopy.

The orientation parameter $\langle\sin^2\theta\rangle$ of the crystallites along the principal axis of a fiber is defined by the equation [25].

$$\left\langle \sin^2\theta \right\rangle = \frac{\int_0^{\pi/2} \rho(\theta)\sin^3\theta \mathrm{d}\theta}{\int_0^{\pi/2} \rho(\theta)\sin\theta \mathrm{d}\theta} \tag{2}$$

where θ is the misorientation angle relative to the fiber axis and $\rho(\theta)$ is the distribution of the 110 reflection, determined by the azimuthal intensity data fitted with a Lorentz function (Fig. 4c). In this model, fibers are considered to be consisting of multiple and parallel aligned chains in which crystallites exhibit a narrow orientation distribution relative to their axis. This method has been used to determine the orientation parameter for single PBO (poly-p-phenylene benzobisoxazole) fibers [26]. For a perfect crystalline orientation, $\langle\sin^2\theta\rangle$ is equal to zero; crystalline orientation is therefore inversely proportional to the value of the orientation parameter, i.e. increasing the degree of crystallite orientation decreases the value of the orientation parameter. The $\langle\sin^2\theta\rangle$ values for Ioncell fibers are shown in Fig. 4d as a function of draw ratio. As

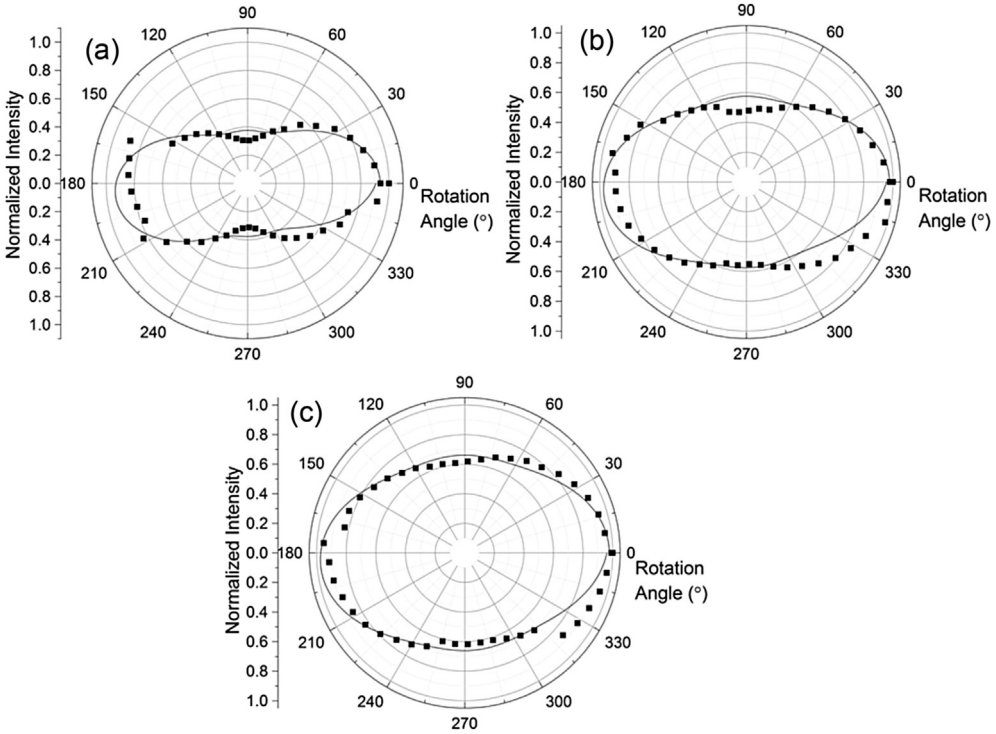

Fig. 3. Normalized intensity of the Raman peak located at ~1095 cm^{-1} as a function of the angle between the polarization direction of the incident laser and the axis of Ioncell cellulose fibers produced using draw ratios (a) 1, (b) 6 and (c) 15. Solid lines are the best fits to the data using Equation (1).

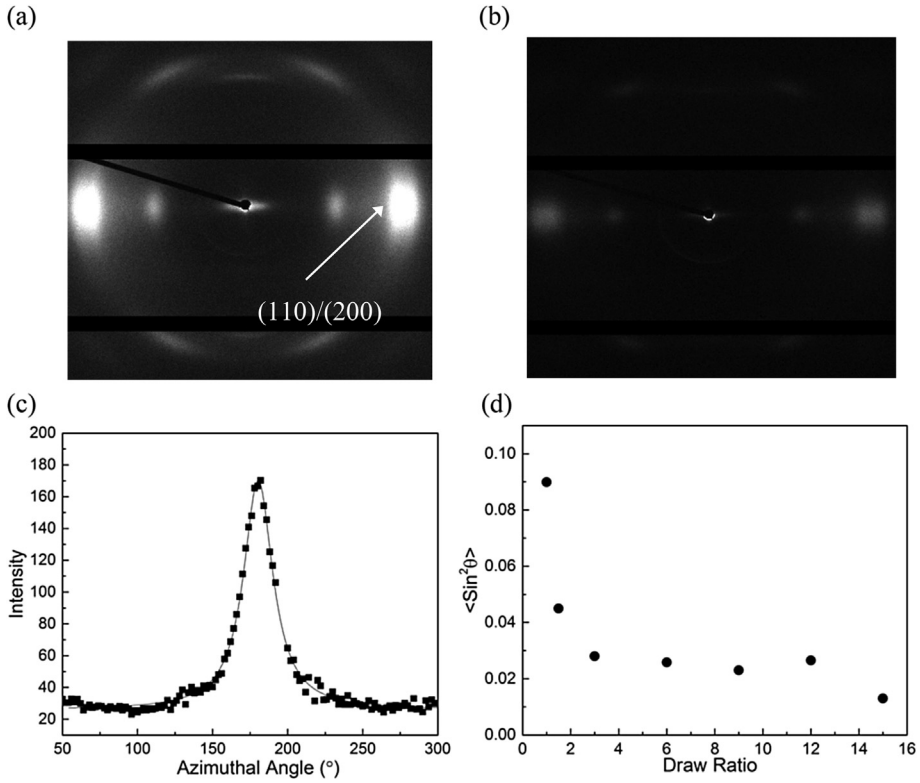

Fig. 4. Typical Wide Angle X-ray Diffraction (WAXD) patterns of Ioncell fibers produced with draw ratios (a) 1.5 and (b) 15; (c) A typical azimuthal intensity plot of the 110 reflection with a fitted Lorentz function (solid black line) and (d) the orientation distribution parameter ($\langle \sin^2\theta \rangle$) as a function of draw ratio.

expected, the orientation distribution parameter decreases with an increase in draw ratio indicating a higher crystalline orientation for fibers produced using higher draw ratios. The orientation parameter for the Ioncell fiber produced using the highest draw ratio (DR = 15; $<\sin^2\theta> = 0.016$) is similar to a value reported for another high performance regenerated cellulose produced from a liquid crystalline cellulose solution (~0.011) [12]. Calculations based on the X-ray diffraction data from a bundle of fibers revealed a slightly lower $\langle \sin^2\theta \rangle$ value of 0.013 for a draw ratio of 15. As a comparison, lyocell cellulose fibers exhibited a much higher orientation parameter of 0.05 at the center of the fiber with a draw ratio of 8.9, implying a lower crystalline orientation along the axis of the fibers [27]. Ioncell fibers' orientation parameter is similar to a value reported for poly (ρ-phenylene terephthalamide) fibers (0.016) [25].

3.2. Mechanical properties of fibers

The mechanical properties of single Ioncell fibers were investigated by uniaxial tensile testing of single filaments. Fig. 5 reports typical stress-strain curves for Ioncell fibers produced using different draw ratios. As shown in Table 1, a significant two-fold increase of Young's modulus was observed for fibers produced using a draw ratio of 6, compared to filaments produced with a draw ratio of 1; further increases in modulus are minimal beyond a draw ratio 6. The elongation-at-break is also noted to decrease with an increasing draw ratio. Tensile strength also plateaus after a draw ratio of 6. The modulus and tensile strength values suggest that a draw ratio of 6 is optimal for obtaining high mechanical properties. The yielding point for the fibers are observed to be about 1.5% strain for all draw ratios and this could have been resulted from the breakdown of hydrogen bonding as reported for other regenerated cellulose fibers [9].

The mechanical properties of these fibers compare favorably with other forms of regenerated cellulose. Ioncell fibers produced with the highest draw ratio (DR = 15) have a higher elastic moduli and tensile strength than Lyocell, CordenkaTM 1840, CordenkaTM 700 and Enka Viscose [11]. These regenerated cellulose fibres exhibit non-linear stress-strain curves similar to that of Ioncell fibers. There is some strain-hardening behavior noted in the stress-strain curves of these samples as also seen in Ioncell fibers (for

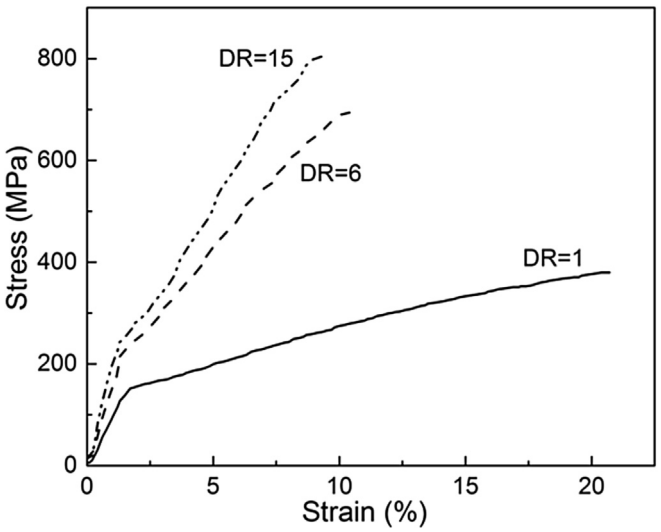

Fig. 5. Typical stress-strain curves of Ioncell fibers produced using different draw ratios.

Table 1
Tensile properties of Ioncell fibers produced using a range of draw ratios (DR). All errors (±) are standard deviations from the mean.

DR	Linear density (dtex)	±	Tensile strength (MPa)	±	Strain (%)	±	Modulus (GPa)	±
1.0	18.64	1.76	354.45	27.01	20.88	2.78	9.5	1.2
1.5	11.11	0.86	464.25	28.96	14.27	1.34	13.6	1.7
3.0	6.52	0.52	576.30	47.87	11.36	1.98	17.8	3
6.0	3.26	0.36	700.80	38.12	10.47	0.6	19	1.6
9.0	2.28	0.29	725.10	24.31	10.5	0.66	20.2	2.7
12.0	1.65	0.19	703.80	34.52	9.22	1.03	21.4	3.8
15.0	1.33	0.17	784.20	55.53	8.88	0.85	23	2.4

higher draw ratios). Elongation-at-break of Ioncell fibers (DR = 15) were higher than that of Lyocell fibers (7%), however, was lower than CordenkaTM fibers (12.7% for CordenkaTM 1840 and 10.7% for CordenkaTM 700) [11].

3.3. Molecular deformation

Shifts in the position of the Raman peak initially located at ~1095 cm^{-1} were followed with tensile deformation of the fibers to gain insight into their molecular deformation. A typical Raman band shift obtained for a single Ioncell fiber is shown in Fig. 6a. Shifts of this type occur due to direct deformation of the molecular backbone bonds, such as C—O—C, as a consequence of macroscopic deformation of the fibers. Fig. 6b shows a typical shift in the peak position of the Raman band initially located at ~1095 cm^{-1} as a function of strain. Raman data in Fig. 6b are fitted with an equation of the form $\Delta\nu = -k_1\varepsilon + k_2\varepsilon^2$ where $\Delta\nu$ is the Raman shift, k_1 and k_2 are constants and ε is strain. This equation is similar in form to the following equation (note: $\Delta\nu$ is negative)

$$\sigma = E\varepsilon - K\varepsilon^2 \tag{3}$$

where σ is the stress, E is the Young's modulus, ε is strain and K is a constant. This equation was first proposed by Nissan [28] for hydrogen-bonded solids such as cellulose and nylon. The use of this equation can be justified since the magnitude of the Raman band shift is shown to be proportional to stress for regenerated cellulose fibers [13]. As the draw ratio used to produce the fibers increases, the Raman band shift rate with respect to strain increases. It is evident from these data that the highest draw ratio fiber (DR = 15) has a strain band shift rate of −1.33 $cm^{-1}\%^{-1}$ which is higher than values previously obtained for a high modulus cellulose fiber produced by a liquid crystalline process (−1.08 $cm^{-1}\%^{-1}$) [12]. For the fibers produced using the lowest draw ratio, the shift rate was much lower (−0.19 $cm^{-1}\%^{-1}$) indicating that the transfer of external deformation to molecular deformation of the cellulose backbone was not dominant in these fibers. This may be explained by a co-chain rotation and shearing between domains as evidenced in other regenerated cellulose fibers with low orientation [9,13]. In comparison, for higher draw ratio fibers, the cellulosic backbone is mostly parallel to the fiber axis and chain stretching is thought to be more dominant. This can be viewed in light of a new model proposed by Bandeira et al. [29] by taking into account the geometry of the crystalline chain slip mechanism, which considers affine deformation of the crystalline phase in the longitudinal drawing direction. This model was based on the work of Ritchie [30] on large strain deformation of polyethylene. The main assumption of this work is that only chain slip along directions parallel to the direction of the chains occurs in the process of crystalline deformation and orientation [30]. Upon applied deformation, the crystalline domains in the material are assumed to slide over one another along slip planes undergoing rotation and displacement in the process; the macroscopic fiber however remains parallel to the loading axis. This model is described by the equation

$$\langle P_2\rangle = \frac{\lambda^2 - 1}{\lambda^2} \tag{4}$$

where $\langle P_2\rangle$ is Hermans' orientation parameter and λ is the draw ratio. Hermans' orientation parameter is also defined by the equation

$$\langle P_2\rangle = \frac{3\langle\cos^2\theta\rangle - 1}{2} \tag{5}$$

where $\langle\cos^2\theta\rangle$ is the average cosine square of the angles between

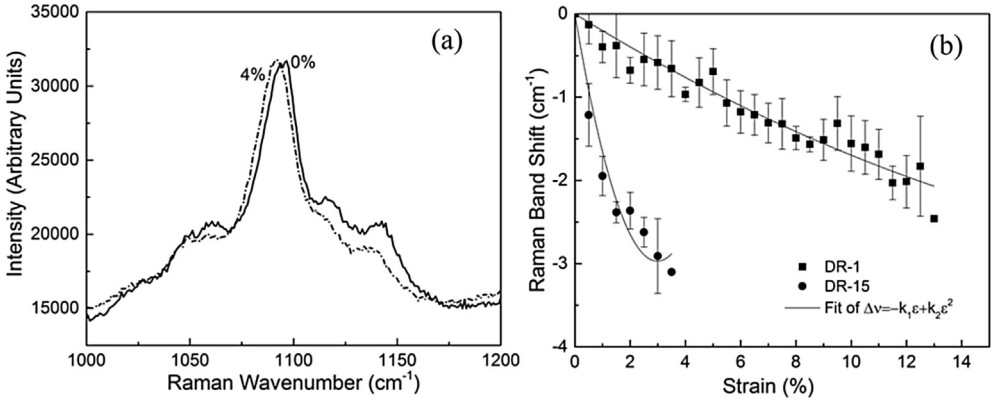

Fig. 6. Typical (a) shift in the Raman band initially located at ~1095 cm^{-1} for single fibers produced using a draw ratio of 9 (strain = 4%) and (b) Raman band shifts as a function of strain for fibers produced using draw ratios of 1 and 15. The solid lines are fits of Equation $\Delta\nu = -k_1\varepsilon + k_2\varepsilon^2$ to the data.

the oriented molecular chains and the drawing direction. Values of Hermans' orientation parameter range from −0.5 for crystals oriented perpendicular to the fiber axis (drawing direction) to unity for crystals oriented parallel to the drawing direction. As shown in Fig. 7, the model (equation (4)) predicts an increase of orientation with an increase of draw ratio and this agrees well with the Hermans' orientation [31] values calculated for Ioncell fibers at higher draw ratios. It should be noted that the model does not agree well with the orientation values for lower draw ratios. The model assumes that an overall increase in crystal length in the fiber axis direction to be the same as the increase in length of the fiber itself and this may not be the case for fibers with low draw ratios. As discussed earlier, Raman data on molecular deformation suggest a co-chain rotation between domains may be dominant for lower draw ratios [9,13], which may not translate into affine deformation along the fiber axis direction as assumed by the chain slip model. Hermans' orientation parameter values represent crystalline orientation since it is obtained from X-ray diffraction data in this case. The close fit between the model and orientation values indicates that crystalline deformation is dominant along the drawing direction for fibers produced using higher draw ratios.

The mechanical properties of Ioncell fibers could be related to their microstructure. Northolt [25,32] proposed a model based on a series aggregate structure for the deformation of high performance rigid-rod polymer fibers, according to the equation

$$\frac{1}{E_f} = \frac{1}{E_c} + \frac{\langle \sin^2 \theta \rangle}{2g} \tag{6}$$

where E_f, E_c, $\langle \sin^2\theta \rangle$ and g are the fiber modulus, crystal modulus, crystalline orientation function, and shear modulus, respectively. As shown in Fig. 8, Equation (6) is in good agreement with the data ($R^2 = 0.97$), and the fit yields a gradient of 0.854 $GPa^{-1}$and an intercept of 0.030 GPa^{-1}. These parameters can be used to derive the crystal modulus and shear modulus, which are found to be 33.3 GPa and 0.585 GPa, respectively. These parameters were also calculated using the X-ray diffraction data from a bundle of fibers (see Supplementary Information); values of 35.7 GPa and 0.454 GPa were obtained for the crystal and shear moduli respectively. The crystal modulus value obtained here are both significantly lower than crystal moduli (77–163 GPa) obtained from other studies on cellulose-II fibers [33]. A model that takes into better account the molecular deformation of the fibers is therefore required.

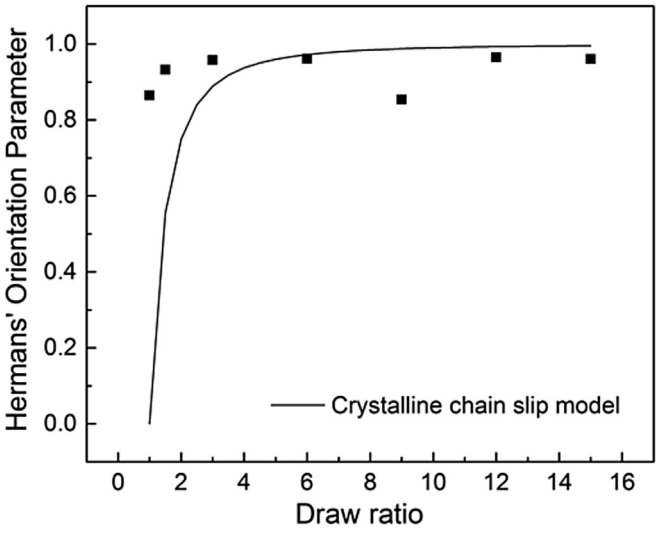

Fig. 7. Hermans' orientation parameter values as a function of draw ratio. The solid line represents the crystalline chain slip model according to Equation (4).

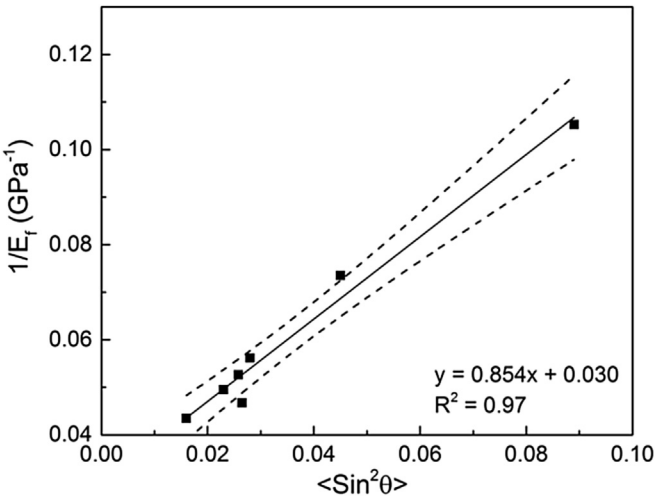

Fig. 8. Reciprocal of the fiber modulus as a function of the crystalline orientation parameter. Solid line is a linear regression to the data, from which parameters (E_c and g) from Equation (6) can be determined. The area enclosed by the dotted lines show the 95% confidence bands for the fit.

If we assume the fibers have a series aggregate structure, then the Raman band shift rate is proportional to the elastic modulus (E_f) of the fibers as shown below

$$\frac{d\nu}{d\varepsilon} \propto E_f = kE_f \tag{7}$$

where $d\nu/d\varepsilon$ is the Raman band shift rate with respect to strain. The value of k was found to be 0.0365 $cm^{-1}\%^{-1}$ GPa^{-1} from a fit to the Raman band shift rate vs E_f data, as shown in Fig. 9a. It is clear that this relationship only holds for the first three data points, which may be because the model only applies to fibres with a low draw ratio. At higher draw ratios though it has been noted that the moduli of regenerated cellulose fibres tend to plateau, which leads to some clustering of the data in Fig. 9a.

By combining Equations (6) and (7) the equation

$$\frac{1}{d\nu/d\varepsilon} = \frac{1}{kE_c} + \frac{\langle \sin^2 \theta \rangle}{2gk} \tag{8}$$

is obtained. As shown in Fig. 9b, a linear fit to these data should give a gradient of $1/2gk$ and an intercept on the y-axis of $1/kE_c$ according to Equation (8). From these fitted values, the crystal modulus is found to be 83 GPa and a value of 0.22 GPa is found for the shear modulus. Crystal moduli values reported in the literature are in the range of 77–163 GPa for cellulose II from both experiment and theory [33]. Our value appears to be in good agreement with this range, and most experimental values (88 GPa, 130 GPa) [34,35], suggesting that this approach possibly takes closer account of chain deformation compared to that of Northolt [25]. It is worth noting that Northolt's theory (in Equation (6)) works well for rigid rod polymer fibers, such as poly (ρ-phenylene terephthalamide), where rotation and chain slip are not thought to be dominant. However, the shear modulus value we obtained is much lower than the range of values ($2.4 \leq g \leq 3.8$ GPa) for a liquid crystalline cellulose fiber [26,32]. The calculations based on X-ray diffraction data from fiber bundles revealed significantly lower values of 58.3 GPa and 0.173 GPa for crystal and shear modulus, respectively. These lower

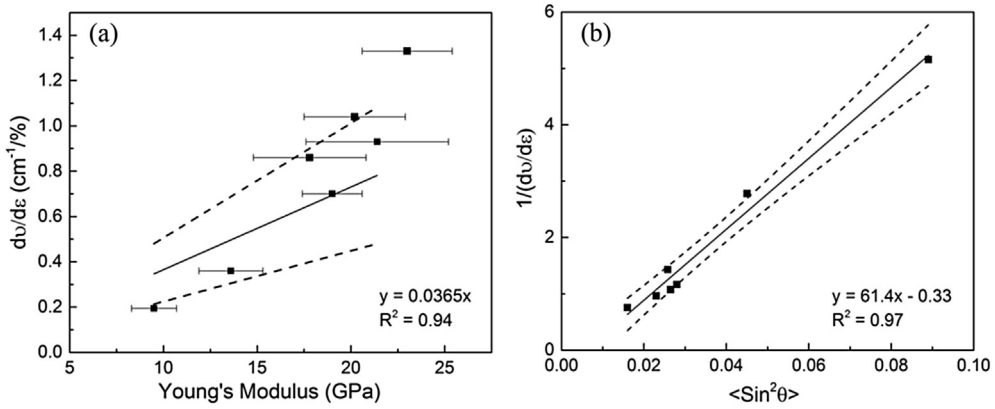

Fig. 9. (a) Raman band shift rate ($d\nu/d\varepsilon$) as a function of Young's modulus and (b) reciprocal Raman band shift rate as a function of $\langle sin^2\theta \rangle$. Solid lines are linear regressions to the data: in (a) the intercept is set to zero and only the first 3 data are included in the regression. The dotted lines are the 95% confidence intervals for the linear regressions.

moduli values may be attributed to the errors involved from fibers that may not be straight within the bundles; indeed the $\langle \sin^2\theta \rangle$ values for the bundles are on average higher than single fibers suggesting some misorientation of filaments.

The reason why such a low value of the shear modulus is obtained, relative to other fibers of similar microstructure (e.g. lyocell, Bocell) is unknown. It may be that chain slip is a dominant mechanism for these fibers, with a breakdown in the intra-chain hydrogen being a mechanism leading to this.

4. Conclusions

An investigation into the molecular deformation and crystal orientation of a new class of regenerated cellulose fibers, produced from an ionic liquid solvent spinning system, was conducted. Raman spectroscopy was used to map the orientation of molecules relative to the long axis of the fiber by monitoring the change in the intensity of the Raman band located at ~1095 cm^{-1}. It was revealed that an intensity ratio that relates to the axial orientation of cellulose molecules (I_{0°/I_{90°) is higher for fibers produced using a low draw ratio, indicative of a skin-core structure to the fibers. X-ray diffraction was used to characterize the crystal orientation of fibers by calculating the orientation distribution parameter $\langle \sin^2\theta \rangle$ that decreases with an increase in draw ratio implying higher orientation of crystals for fibers with higher draw ratios. Tensile testing of Ioncell fibers revealed that when the fiber draw ratio is increased from 1 to 6, a two-fold increase of Young's modulus and tensile strength was observed. Raman spectroscopy was used to show that the shift rate with respect to strain of a band initially located at ~1095 cm^{-1} increases with the draw ratio of the fibers, indicative of an increase in the molecular deformation of cellulose chains along the fiber axis. A crystalline chain slip model was used to predict the increase of Hermans' orientation parameter values with an increase of draw ratio. Good agreement was found between the model and the data, which is indicative of the dominant crystalline affine deformation along the longitudinal fiber axis. A model inclusive of both molecular and crystal deformation was used to predict the crystal modulus (83 GPa), which is in agreement with other experimental values. However, the shear modulus was found to be significantly lower than other studies (at 0.22 GPa). The reason behind such a low value may be due to chain slip being a dominant mechanism during deformation, but this may require further investigation.

Acknowledgements

The Engineering and Physical Sciences Research Council (EPSRC) is acknowledged for funding provided under Grant No. EP/L017679/1.

Appendix A. Supplementary data

Supplementary data related to this article can be found at http://dx.doi.org/10.1016/j.polymer.2016.07.007.

References

[1] C.F. Cross, E.J. Bevan, C. Beadle, Improvements in dissolving cellulose and allied compounds. British Patent 8, 700, 1892.
[2] R.P. Swatloski, S.K. Spear, J.D. Holbrey, R.D. Rogers, Dissolution of cellulose with ionic liquids, J. Ame. Chem. Soc. 124 (2002) 4974–4975.
[3] L.K.J. Hauru, M. Hummel, A. Michud, H. Sixta, Dry jet-wet spinning of strong cellulose filaments from ionic liquid solution, Cellulose 21 (2014) 4471–4481.
[4] A. Michud, M. Tanttu, S. Asaadi, Y. Ma, E. Netti, P. Kaariainen, A. Persson, A. Berntsson, M. Hummel, H. Sixta, Ioncell-F: ionic liquid-based cellulosic textile fibers as an alternative to viscose and lyocell, Text. Res. J. 86 (2016) 543–552.
[5] H. Sixta, A. Michud, L. Hauru, S. Asaadi, Y. Ma, A.W.T. King, I. Kilpeläinen, M. Hummel, Ioncell-F: a high-strength regenerated cellulose fibre, Nord. Pulp Pap. Res. J. 30 (2015) 43–57.
[6] W. Gindl, K.J. Martinschitz, P. Boesecke, J. Keckes, Orientation of cellulose crystallites in regenerated cellulose fibres under tensile and bending loads, Cellulose 13 (2006) 621–627.
[7] W. Gindl-Altmutter, S.J. Eichhorn, M. Burghammer, J. Keckes, Radial crystalline texture in a lyocell fibre revealed by synchrotron nanofocus wide-angle X-ray scattering, Cellulose 21 (2013) 845–851.
[8] K. Kong, M.A. Wilding, R.N. Ibbett, S.J. Eichhorn, Molecular and crystal deformation of cellulose: uniform strain or uniform stress? Faraday Discuss. 139 (2008) 283.
[9] K. Kong, S.J. Eichhorn, The influence of hydrogen bonding on the deformation micromechanics of cellulose fibers, J. Macromol. Sci. Phys. 44 B (2005) 1123–1136.
[10] S.J. Eichhorn, R.J. Young, Deformation processes in regenerated cellulose fibers, Cellulose 8 (2001) 197–207.
[11] S.J. Eichhorn, J. Sirichaisit, R.J. Young, Deformation mechanisms in cellulose fibres, paper and wood, J. Mater. Sci. 36 (2001) 3129–3135.
[12] S.J. Eichhorn, R.J. Young, R.J. Davies, C. Riekel, Characterisation of the microstructure and deformation of high modulus cellulose fibres, Polymer 44 (2003) 5901–5908.
[13] K. Kong, S.J. Eichhorn, Crystalline and amorphous deformation of process-controlled cellulose-II fibres, Polymer 46 (2005) 6380–6390.
[14] V.K. Mitra, W.M. Risen, R.H. Baughman, A laser Raman study of the stress dependance of vibrational frequencies of a monocrystalline diacetyline, J. Chem. Phys. 66 (1977) 2731–2736.
[15] R.J. Young, Monitoring deformation processes in high-performance fibres using Raman spectroscopy, J. Text. I. 86 (1995) 360–381.
[16] T. Pullawan, A.N. Wilkinson, S.J. Eichhorn, Orientation and deformation of wet-stretched all-cellulose nanocomposites, J. Mater. Sci. 48 (2013) 7847–7855.

[17] R.H. Atalla, S.C. Nagel, Cellulose: its regeneration in the native lattice, Science 185 (1974) 522–523.
[18] J.H. Wiley, R.H. Atalla, Band assignments, in the Raman spectra of celluloses, Science 160 (1987) 113–129.
[19] H.G. Edwards, D.W. Farwell, D. Webster, FT Raman microscopy of untreated natural plant fibres, Spectrochim. Acta. A 53A (1997) 2383–2392.
[20] C.E. Moss, M.F. Butler, M. Muller, R.E. Cameron, Microfocus small-angle X-ray scattering investigation of the skin-core microstructure of lyocell cellulose fibers, J. Appl. Polym. Sci. 83 (2002) 2799–2816.
[21] J. Sundberg, V. Guccini, K.M.O. Hakansson, G. Salazar-Alvarez, G. Toriz, P. Gatenholm, Controlled molecular reorientation enables strong cellulose fibers regenerated from ionic liquid solutions, Polymer 75 (2015) 119–124.
[22] T. Cai, H. Zhang, Q. Guo, H. Shao, X. Hu, Effects of expandable graphite and modified ammonium polyphosphate on the flame-retardant and mechanical properties of wood flour-polypropylene composites, J. Appl. Polym. Sci. 115 (2009) 1047–1053.
[23] K. Kong, L. Deng, I.A. Kinloch, R.J. Young, S.J. Eichhorn, Production of carbon fibres from a pyrolysed and graphitised liquid crystalline cellulose fibre precursor, J. Mater. Sci. 47 (2012) 5402–5410.
[24] Z. Li, R.J. Young, I.A. Kinloch, Interfacial stress transfer in graphene oxide nanocomposites, ACS Appl. Mater. Interfac. 5 (2013) 456–463.
[25] M.G. Northolt, Tensile deformation of poly(p-phenylene terephthalamide) fibres, an experimental and theoretical analysis, Polymer 21 (1980) 1199–1204.
[26] R.J. Davies, M.A. Montes-Morán, C. Riekel, R.J. Young, Single fibre deformation studies of poly (p-phenylene benzobisoxazole) fibres, J. Mater. Sci. 38 (2003) 2105–2115.
[27] K. Kong, R.J. Davies, M.A. McDonald, R.J. Young, M.A. Wilding, R.N. Ibbett, S.J. Eichhorn, Influence of domain orientation on the mechanical properties of regenerated cellulose fibers, Biomacromolecules 8 (2007) 624–630.
[28] A.H. Nissan, The rheological behaviour of hydrogen-bonded solids, Trans. Faraday Soc. (1956) 700–709.
[29] B. Bandeira, E.L.V. Lewis, D.C. Barton, I.M. Ward, The degree of crystalline orientation as a function of draw ratio in semicrystalline polymers: a new model based on the geometry of the crystalline chain slip mechanism, J. Mater. Sci. 51 (2016) 228–235.
[30] S.J.K. Ritchie, Model for the large-strain deformation of polyethylene, J. Mater. Sci. 35 (2000) 5829–5837.
[31] C.P. Lafrance, M. Pezolet, R.E. Prud'homme, Study of the distribution of molecular orientation in highly oriented polyethylene by x-ray diffraction, Macromolecules 24 (1991) 4948–4956.
[32] M.G. Northolt, H. Boerstoel, H. Maatman, R. Huisman, J. Veurink, H. Elzerman, The structure and properties of cellulose fibers spun from an anisotropic phosphoric acid solution, Polymer 42 (2001) 8249–8264.
[33] S.J. Eichhorn, R.J. Young, G.R. Davies, Modeling crystal and molecular deformation in regenerated cellulose fibers, Biomacromolecules 6 (2005) 507–513.
[34] J. Mann, X-ray measurements of the elastic modulus of cellulose crystals, Polymer 3 (1962) 549–553.
[35] R.J. Young, S.J. Eichhorn, Deformation mechanisms in polymer fibres and nanocomposites, Polymer 48 (2007) 2–18.

2016-07-05

Deformation mechanisms in ionic liquid spun cellulose fibers

Wanasekara, Nandula D.

Elsevier

Nandula D. Wanasekara, Anne Michud, Chenchen Zhu, et al., Deformation mechanisms in ionic liquid spun cellulose fibers. Polymer, Volume 99, 2 September 2016, Pages 222-230
https://doi.org/10.1016/j.polymer.2016.07.007